Climatology of Extreme Rainfall over China with Hourly through 24-Hour Accumulation Periods Based on National-Level Hourly Rain Gauge Data

Yongguang Zheng[1], Ming Xue[2, 3], Bo Li[4], Jiong Chen[1], Zuyu Tao[5]

[1]National Meteorological Centre, Beijing 100081, China
[2]School of Atmospheric Sciences, Nanjing University, Nanjing, China
[3]Center for Analysis and Prediction of Storms, Oklahoma University
[4]University of Illinois at Urbana-Champaign
[5]Peking University, Beijing 100871, China

Revised, February, 2016

Submitted to Journal of Applied Meteorology and Climatology
April 2015

Corresponding author

Ming Xue
Center for Analysis and Prediction of Storms, Oklahoma University
mxue@ou.edu

ABSTRACT

Hourly rainfall measurements of 1919 national-level meteorological stations from 1981 through 2012 are used to document, for the first time, the climatology of extreme rainfall at hourly through daily accumulation periods in China. Rainfall at 3-, 6-, 12-, and 24-h periods are constructed through running accumulation from hourly rainfall data at each station with proper quality control. For each station and for each accumulation period, the historical maximum is found, and the corresponding 50-year return values are estimated using the generalized extreme value theory. Based on percentiles of extreme rainfall values among all the stations, standard thresholds separating Grade I, Grade II and Grade III extreme rainfall are established, which roughly correspond to the 70th and 90th percentiles for each of the accumulation periods.

The spatial distributions of the two types of extreme rainfall are then examined for different accumulation periods. The spatial distributions of extreme rainfall at hourly through 6-h periods are more similar than those of 12- and 24-h periods. Grade III rainfall is mostly found over South China, the western Sichuan Basin, along the southern and eastern coast lines, in the large river basins and plains. There are similar number of stations with Grade III extreme hourly rainfall north and south of 30°N, but the percentage increases to about 70% south of 30°N as the accumulation period increases to 24 hours, reflecting richer moisture and more prolonged rain events in southern China. Potential applications of the extreme rainfall climatology and classification standards are suggested at the end.

1. Introduction

Extreme weather and climate events are receiving more and more attention due to their great threat to lives and properties. For example, extremely heavy rainfall can cause human casualties, urban flooding, river overflow, landslides, and other forms of disaster. Extreme weather and climate events are usually defined as low-probability events for particular times and locations, often with a probability of occurrence lower than 10% (e.g., IPCC 2013). Therefore, the probability for an extreme event is usually discussed in terms of percentiles, and the 95th percentile is commonly used as the threshold (e.g., Frich et al. 2002; Zhai et al. 2005). To date, there have been numerous studies on extreme weather and climate events, but most have focused on their detection, spatial distribution, and climate change characteristics (e.g., Frich et al. 2002; Garrett and Müller 2008; Sen Roy 2009). Within China, Zhai et al. (1999, 2005) studied the spatial distributions of extreme daily temperature and rainfall as well as their climatological trends of change, based on a dataset of 349 meteorological stations during 1951–1995 and another dataset of 740 stations during 1951–2000. Gao et al. (2012) detailed the spatial distributions of a number of extreme weather and climate events in China, including the extreme daily and 3-day precipitation, using a dataset from 1031 meteorological stations in China during 1951–2011.

Due to the lack of availability of long-term hourly rainfall data in China (Fig. 1), there exists hardly any research on extreme rainfall for accumulation periods shorter than 24 hours prior to 2010. Hourly rainfall of $\geq$ 20 mm is commonly referred to as a short-duration heavy rainfall (SDHR) event, which is rare in China and the United States (Davis 2001; Zhang and Zhai 2011; Chen et al. 2013). Zhang and Zhai (2011) presented the temporal and spatial distributions and climate changes of extreme hourly rainfall with intensities greater than 20 mm h^{-1} and 50 mm h^{-1}.

The study focused on central and eastern China for May–September, using hourly rainfall data from 480 meteorological stations during 1961–2000. Chen et al. (2013) documented the temporal and spatial characteristics of SDHR events of no less than 10, 20, 30, 40 and 50 mm per hour over China during April–September using hourly rainfall data from 549 stations for 1991–2009. Neither study analyzed the spatial distributions of extreme rainfall for different return periods of hourly rainfall, however. Using the probability distribution of generalized extreme value (GEV, Coles 2001) and based on hourly rainfall data from 465 and 321 stations in China, respectively, Li et al. (2013a, 2013b) presented the return values and their spatial characteristics for 2-, 5-, 10-, and 50-yr return periods. However, they did not examine and analyze in detail the differences among extreme rainfall for accumulation periods from hourly to 24 hours. Despite those existing investigations, a few concerns remain:

(1) The meteorological station data used in previous studies were all very sparse, with the number of stations considered usually less than 600, so those studies may not fully capture extreme rainfall events produced by mesoscale or convective scale systems.

(2) There has been no study on the spatial distributions of extreme rainfall at accumulation periods between 1 and 24 hours in China. Furthermore, no published study has compared the spatial distributions of extreme rainfall at accumulation periods ranging from 1 to 24 hours.

(3) Previous studies on extreme precipitation in China either focused on daily or hourly rainfall (e.g., Zhai et al. 1999, 2005; Gao et al. 2012; Li et al. 2013a, 2013b); the 3-, 6-, 12- and 24-h running cumulative rainfall amounts have not been examined. The use of daily rainfall, rather than 24-hour running accumulation, may underestimate extreme rainfall that straddles the recording day.

(4) There is thus far no classification standard, based on statistically determined thresholds,

for extreme rainfall at different accumulation periods in China.

Because the occurrence of extreme rainfall at any single meteorological station carries a very low probability, the prediction of such highly improbable events is very difficult. However, if a dataset from a large number of meteorological stations covers a sufficiently long time period, it is possible to estimate the distributions of extreme events and thereby provide useful information for improving the prediction of such rare events. For these reasons, utilizing hourly rainfall data at 2420 national-level meteorological stations in China that cover 1951–2012, we document and investigate the spatial distributions of two types of extreme rainfall, the historical maximum and the estimated 50-yr return value (hereafter 50-yr rainfall), for running accumulation periods of 1, 3, 6, 12, and 24 hours. Based on such long-term historical data covering a large portion of China, we establish standards of classification for extreme rainfall, in terms of threshold values that separate three grades of extreme rainfall, for different accumulation periods. The thresholds roughly correspond to 70 and 90 percentiles of extreme rainfall distributions. Our study allows us to classify different regions based on their extreme rainfall, and it also provides important reference information for the estimation and prediction of extreme rainfall in China (Fig. 1).

In the rest of this paper, we first describe the data and analysis methods used. In sections 3 and 4, we document and discuss the spatial distributions of historical rainfall maxima and 50-yr return values, respectively. Section 5 examines the regional distributions of extreme rainfall. Summary and conclusions are given in section 6.

2. Data and Methods

a. Data

The hourly rainfall dataset (HRD) during 1951–2012 was obtained from the National

Meteorological Information Center of the China Meteorological Administration. In this dataset, the rainfall was measured by either tipping-buckets or self-recording siphon rain gauges, or from automatic rain gauges, at 2420 national-level meteorological stations in contiguous China. The data were subject to strict quality control by the data provider according to the following rules. For each individual rain gauge at any single day, the difference between the observed daily rainfall and the accumulated daily value from hourly rainfall is calculated. The hourly rainfall data are considered erroneous if this difference exceeds a threshold: For daily rainfall $\geq$ 5 mm the threshold is 20% of the daily amount and for daily rainfall < 5 mm the threshold is 1 mm. All erroneous data were discarded in this study.

The number of meteorological stations available in the HRD increased over the years. In the 1950s, there were less than 1000 stations but the number increased to more than 2000 after 1980. The number of stations taking observations in July is around two to three times greater than that of January, because a number of stations in northern China routinely stop taking rainfall measurement in the freezing conditions of the winter season under certain regulations. In general, the densest observations occur in the central and eastern China. Although the spatial and temporal coverages of the HRD are not homogeneous, this dataset represents the most complete and accurate measurements of hourly rainfall in China to date.

For identifying extreme rainfall data series that cover the same climatological periods over China, we only select the stations that have at least 25 hourly-rainfall-observation days in the summer months (June, July and August) of each year. The reason for this screening is that China is significantly affected by the East Asian summer monsoon and thus heavy rain and SDHR events mainly occur in summer (Ding and Zhang 2009; Chen et al. 2013). In the end, 783 stations with continuous observations were selected for the period of 1965–2012 and 1919 stations were selected for the period of 1981–2012, with the former being a subset of the latter (Fig. 1b). The average distance between the 1919 stations is about 50 km. The selected stations are mainly located in the central and eastern China east of 100°E, and only a few stations are situated in the Tibetan Plateau or in the western deserts, west of 100°E (Fig. 1b).

To better capture the extreme sub-daily rainfall events, our study uses all available rainfall data from the 1919 stations for the period of 1981–2012 to get the historical maximum and estimate the 50-yr return value at each station. Given that the observational periods of the 1919 stations cover more than 30 years, the rainfall data from these stations are regarded as carrying sufficient climatological information. To obtain the historical maximum rainfall series at different accumulation periods for each station, we first compute the running 3-, 6-, 12- and 24-h cumulative rainfall from hourly rainfall data, we then find the historical rainfall maximum for each accumulation period from the complete series. This ensures a full account of extreme rainfall that straddles the rainfall accumulation periods. We obtained the spatial distributions of the historical rainfall maximum for both the 1965–2012 and 1981–2012 periods, and we find that the spatial distributions from the two periods are similar for all accumulation periods, although their rainfall amounts are somewhat different. We will show results from the latter period only because it has more stations.

Different regions of China will be referred to in this paper. Figure 1a labels provinces and 4 main rivers of China, while Fig. 1b divides and labels various regions. For brevity, we use term “Northeast China” to refer to the provinces of Heilongjiang, Jilin and Liaoning. “North China” includes the cities of Beijing and Tianjin, and the provinces of Hebei and Shanxi, and “South China” comprises the provinces of Guangxi, Guangdong, and Hainan.

b. GEV distribution and estimation

The historical maximum rainfall series at different accumulation periods at each station are considered random processes of extremes, we therefore use the GEV distribution to model the annual maxima, and then estimate the 50-yr rainfall amount for each station. The GEV distribution has been widely applied to extreme rainfall estimation (e.g., Coles 2001; Gao et al. 2012; Li et al. 2013a, 2013b). The 50-yr rainfall is considered an extreme event according to the definition of extreme weather and climate events (e.g., IPCC 2013). According to the probability theory, for an event with a 50-yr return period, the probability of at least one such occurrence in 50 years is 63.6% (Atomic Energy Regulatory Board of India 2008).

The GEV cumulative probability distribution is defined as

$$G(z) = \exp\left\{-\left[1 + \xi\left(\frac{z-\mu}{\sigma}\right)\right]^{-1/\xi}\right\}, \quad (1)$$

where $G(z)$ is the probability that z is not exceeded, and μ, σ and ξ are the location, scale and shape parameters, respectively. The parameters must satisfy $1 + \xi(z-\mu)/\sigma > 0$, $-\infty < \mu < \infty$, $\sigma > 0$ and $-\infty < \xi < \infty$ (Coles 2001). Given an annual maximum sample series, one can estimate the parameters and then determine the cumulative probability function of the GEV either using the maximum likelihood method (Coles 2001) or the L-moments method (Hosking 1990). We choose the maximum likelihood method in our estimation. After obtaining the annual maximum rainfall series for a given accumulation period and a given station, we estimate parameters μ, σ and ξ of the GEV distribution, assuming the series is stationary. With the estimated GEV distribution function, we then estimate the rainfall amounts for different return periods.

Two stations, Beijing in North China and Qingyuan in South China, are taken from those 783 stations for the period of 1965–2012 as examples to show the reliability of the estimated GEV distribution function. The reason for choosing these two stations is because they both have relatively longer observational periods and also represent different climate regions. For brevity, we show in Figs. 2 and 3 only the probability plots, the fitted GEV distributions and the 95% confidence intervals of hourly and 24-h rainfall, for the two stations respectively, in order to evaluate the goodness-of-fit of the fitted model.

The fitted GEV distributions using the hourly, 3-, 6-, 12-, and 24-h rainfall data of 1965–2012 and of 1981–2012 (in Figs. 2 and 3, respectively, but without showing the fitted GEV distributions of 3-, 6-, and 12-h rainfall) all agree with the probability distributions of annual rainfall maxima well. The fitted probability distributions using the two datasets are very similar. The confidence intervals for the estimated return level curves are wider for longer return periods, in particular for return periods longer than 50 years, which is not surprising. Therefore, in section 4, we will only present the spatial distributions of estimated 50-yr rainfall return level, although all rainfall events with return periods no shorter than 50 years are considered extreme. In addition, due to different lengths of the two datasets used, some differences between the fitted GEV distributions are also seen. The 50-yr rainfall amounts from the fitted GEV distribution using the 1981–2012 dataset are higher than those using the 1965–2012 dataset, which may be related to the fact that the observational period of the former dataset is shorter and the dataset features on average heavier rainfall amounts.

The reliability of the estimated 50-yr rainfall across China is also tested by comparing the spatial distributions of the two estimates from the two datasets; and they are found to be consistently similar for all different accumulation periods.

c. Classification of extreme rainfall

There is thus far no standard classification in China that is particularly designed for extreme rainfall at different accumulation periods; and all existing classifications are based on fixed amounts of rainfall regardless of their accumulation periods. Rainfall amounts with different accumulation periods cannot be directly compared. We propose in this paper to develop a new standard categorization for classifying extreme rainfall according to their accumulation periods, and then further classify different regions based on their extreme rainfall classification. We propose to use the percentiles of the extreme rainfall over the 1919 stations at different accumulation period to define the thresholds of classification. With the establishment of such standard thresholds, the extreme rainfall at different accumulation periods can be classified consistently, thus the spatial distributions of the extreme rainfall at different accumulation periods can be compared with each other, and the differences in extreme rainfall for different accumulation periods among various regions can be obtained.

For the historical maximum or the 50-yr rainfall at any accumulation period during 1981–2012, we first sort the extreme rainfall data series at the 1919 stations (there is only one extreme rainfall value at each station) in an ascending order, then their 70th and 90th percentiles can be easily determined. These values are given separately in Table 1 for the historical maximum and the 50-yr rainfall. As the historical maximum rainfall values differ slightly from their corresponding 50-yr return value, to facilitate the comparison of the spatial distributions between these two types of extreme rainfall and among different rainfall accumulation periods, we compute the threshold values of two levels for the extreme hourly, 3-, 6-, 12- and 24-h rainfall datasets mainly according to the 50-yr rainfall values in Table 1 (see Table 2). Table 2 shows that the threshold values for the low level (to be defined as Grade I precipitation) are located around the 69th percentile of the ordered historical maximum rainfall sequence, and around the 70th percentile of the ordered 50-yr rainfall sequence among the 1919 stations. Thresholds for the high level (to be defined as Grade III precipitation) correspond approximately to the 89th percentile of the ordered historical maximum rainfall sequence, and the 90th percentile of the ordered 50-yr rainfall sequence. Thus three grades of extreme rainfall in Table 3 are proposed to classify and compare the spatial distributions among different types of extreme rainfall. In the following sections, we will use the classification and threshold values defined above to examine the spatial distributions of the extreme rainfall.

We note there that the Central Meteorological Office of China classifies daily rainfall of no less than 50 mm, 100 mm and 250 mm as heavy rainfall, very heavy rainfall, and extremely heavy rainfall, respectively (Ding and Zhang 2009). Therefore, all the thresholds for Grade II and Grade III extreme rainfall at different accumulation periods defined above are much greater than that for the heavy rain threshold (50 mm) defined in China. Furthermore, except for thresholds for Grade II (75 mm) and Grade III (95 mm) extreme hourly rainfall, all other thresholds are greater than that of very heavy rainfall threshold (100 mm). The threshold for Grade III extreme hourly rainfall (95 mm) approaches that of very heavy rainfall (100 mm), and thresholds for Grade III extreme 12-h rainfall (260 mm) and Grade II extreme 24-h rainfall (230 mm) are close to that of extremely heavy rainfall (250 mm). Note that the threshold for Grade III extreme 24-h rainfall (305 mm) is much greater than that of extremely heavy rainfall (250 mm).

d. Spatial distributions of extreme rainfall

For the convenience of contour plotting, we utilize a grid of 0.75° × 0.75° latitude-longitude cells. We identify the maximum extreme rainfall amount within each of the cells for each accumulation period. For each grid cell, the maximum extreme rainfall amount is equal to the highest value among the stations within that grid cell. If no rainfall observation is found within a cell, that cell is assigned a missing value and is not contoured (the cell will be shown as white). Since the average distance among the 1919 stations is about 50 km, the 0.75° grid distance is somewhat greater than the average distance so the use of this grid would smooth the spatial distribution somewhat where station density is high.

The spatial distributions of the historical rainfall maxima and the estimated 50-yr rainfall are shown in Fig. 4 and Fig. 5, respectively, for different accumulation periods. Grades II and III are shown for all periods in dark blue and magenta colors, respectively. The 20 mm threshold is shown for hourly extreme rainfall which corresponds to the definition of SDHR (Chen et al. 2013), while 50 mm is shown for all accumulation periods corresponding to the definition of daily heavy rainfall (Ding and Zhang 2009) in China. In addition, the threshold value of Grade III extreme hourly rainfall (95 mm) is also presented for accumulation periods longer than 1 hour. In addition to the contour maps, stations with Grade II and Grade III extreme rainfall are plotted as green and yellow dots, respectively, in Figs. 4 and 5. While the contour maps are convenient for revealing the spatial distributions, in the next sections we will focus our discussions more on the stations because they are more faithful to the original observations.

As stated in the previous subsections, the spatial distributions of the historical maximum and the estimated 50-yr rainfall for the period of 1965–2012 (not shown) are consistently similar to those for 1981–2012 regardless of their accumulation periods. However, considering that the latter data are taken from more stations, which can provide a finer-scale spatial representation, we only present the latter in this paper.

3. Spatial distributions of historical maximum rainfall

At a given station for a given accumulation period, the historical maximum rainfall represents the most extreme value that has been recorded in the dataset used. Overall, the spatial distributions of historical maximum rainfall are very uneven (Fig. 4). The rainfall amounts over the southern part of China are larger than those over the northern part, over eastern China are larger than over western China, over the coastal areas are larger than over inland areas, over the southern coastal areas are larger than over the northern coastal areas, over the southern inland areas are larger than over the northern inland areas, and over the major plains and river valleys are larger than over the adjacent large plateaus and mountains. This has to do with the warm air and moisture supply, which is the richest from the south and from the ocean. Grade III historical maximum hourly, 3-, 6-, 12-, and 24-h rainfall are most noticeable east and south of the black solid line in each panel of Fig. 4, which runs from southern Liaoning, through northern Hebei, Shanxi, Sichuan, and then to Yunnan Province. The areas with heavier historical maximum rainfall at different accumulation periods are mainly located in the coastal areas of China, South China, the Yangtze and Huai River Basin, the Yellow and Huai River Basin, the western Sichuan Basin, and the North China Plain.

The above spatial distributions share some similarities with those of heavy rainfall and SDHR occurrence frequency (Zhang and Lin 1985; Chen et al. 2013) over the central and eastern China. For example, both South China and the Sichuan Basin (Regions ① and ⑤ in Fig. 1b) exhibit heavier historical maximum rainfall, higher mesoscale convective system (MCS) frequency (Zheng et al. 2008), higher heavy rainfall frequency, and heavier average annual precipitation, than other regions of China. However, the spatial distributions of the historical maximum rainfall differ greatly from those of MCS frequency, heavy rainfall frequency, and average annual precipitation (Zhang and Lin 1985; Zheng et al. 2008; Chen et al. 2013) east of 100°E, especially over the region between 25° N and 40°N, which includes Hunan, Jiangxi, Zhejiang provinces, the Yellow and Huai River Basin, the Shandong Peninsula, and the North China Plain (Fig. 1). For instance, Hunan, Jiangxi, and Zhejiang provinces exhibit higher MCS, heavy rainfall, and SDHR frequency, and heavier average annual precipitation (Zhang and Lin 1985; Zheng et al. 2008; Chen et al. 2013), but they still suffer from less intense historical maximum rainfall than the regions of the Yellow and Huai River Basin, the Shandong Peninsula, and the North China Plain.

West of the thick black line in Fig. 4, most of the historical maximum hourly, 3-, 6-, 12-, and 24-h rainfall amounts attain only Grade I (below 75 mm, 125 mm, 160 mm, 195 mm, and 230 mm, respectively) according to our classification, although most of them are greater than 20 mm, the threshold of SDHR for hourly rainfall. Conversely, east of the line, there are several areas featuring historical maximum hourly, 3-, 6-, 12-, and 24-h rainfall of no less than 95 mm, 155 mm, 205 mm, 260 mm, and 305 mm (Grade III), respectively.

Figure 4 shows that the stations with Grade II historical maximum hourly, 3-, 6-, 12-, and 24-h rainfall are mostly concentrated over South China, the western Sichuan Basin, the eastern Hubei Province, the coastal areas of Zhejiang and Fujian provinces, the Yangtze and Huai River Basin (excluding the central Anhui Province), the Yellow and Huai River Basin, the North China Plain, and the southern Liaoning Province. However, over Guizhou, Hunan, the western Jiangxi, the inland Zhejiang, and the inland Fujian provinces, which are located between 25°N and 30°N, the stations with Grade II rainfall are sparse and scattered, although there are higher occurrence frequencies of SDHR events (Chen et al. 2013) and MCSs (Zheng et al. 2008).

Furthermore, the densely distributed stations with Grade III historical maximum hourly, 3-, 6-, 12-, and 24-h rainfall (Fig. 4) are located mainly over South China, the western Sichuan Basin, the eastern Hubei Province, the coastal area of Zhejiang Province, the northern coastal area of

Fujian Province, the eastern Henan Province, the Yellow and Huai River Basin, the North China Plain, and parts of the southern Liaoning Province. Whereas, over the area north of 30°N in China, the number of stations with Grade III historical maximum 12- or 24-h rainfall (≥ 260 mm or ≥ 305 mm) is significantly fewer than that with Grade III historical maximum hourly and 3-h rainfall (≥ 95 mm and ≥ 155 mm). However, over the eastern and northern Jiangxi Province, there are more stations with Grade III 24-h rainfall than those with Grade III hourly, 3-, 6-, and 12-h rainfall.

For various regions labeled in Fig. 1b, the heaviest rainfall for a region is obtained as the maximum that has ever been recorded at any one station within the region. The heaviest hourly rainfall is above 140 mm over South China, and it is 135 mm and close to 140 mm over the eastern Hubei Province, the Yellow and Huai River Basin, and the southern North China. Therefore, there are only slight regional differences in historical maximum hourly rainfall amounts among the southern North China, the Yellow and Huai River Basin, and South China. However, for the historical maximum 24-h rainfall, the heaviest rainfall is above 550 mm over South China while over the southern North China and the Yellow and Huai River Basin, it is only about 420 mm. Clearly, there are larger differences, in both relative and absolute values, among 24-h extreme rainfall across China than hourly extreme rainfall. This suggests that heavy rainfall events in Southern China are longer-lasting that those in Northern China.

Apart from the spatial distributions of historical maximum rainfall, we are also interested in how the extreme rainfall is distributed in amounts. The most popular amounts of the historical maximum rainfall among the 1919 stations are determined by applying different bin-widths to different accumulation periods. Using 20 mm as the bin-width, stations with hourly extreme rainfall between 60–80 mm are most common and accounts for 40.8% of total stations. Using 50 mm as an interval, stations with 3-h extreme rainfall between 100–150 mm are most common (42.7%); stations with rainfall between 100–150 mm are most common for 6-h extreme rainfall (36.5%); for 12-h extreme rainfall, 150–200 mm amounts are most common (27.7%). Using 100 mm as an interval of 24-h extreme rainfall, amounts between 100–200 mm are most common, accounting for 44.8% of total stations.

4. Spatial distributions of 50-yr return values

This section describes the spatial distributions of 50-yr return values for hourly, 3-, 6-, 12-, and 24-h rainfall obtained from the fitted GEV distribution based on the 1981–2012 data. These spatial distributions are compared to those of the historical maximum rainfall at different accumulation periods.

As given in Table 2, the numbers of stations with Grade II and Grade III 50-yr rainfall for different accumulation periods are less than those with their corresponding historical maximum rainfall. Nevertheless, the spatial patterns of the 50-yr return values for hourly, 3-, 6-, 12-, and 24-hr rainfall are generally similar to those of the corresponding historical maximum rainfall. Similar to Fig. 4, over the areas east and south of the thick black line in each panel of Fig. 5, the estimated 50-yr rainfall return values at some stations can attain Grade III. Figures 5d and 5e clearly show that there are much fewer stations with Grade III 50-yr return values for 12- or 24-h rainfall than those for hourly and 3-h rainfall over the area north of 30°N in China.

Similar to how we get the most popular rainfall amounts in the historical maxima, we also examine the 50-yr return values. With a 20 mm bin-width for hourly rainfall, stations with 60–80 mm rainfall are most common, accounting for 42.4% of all stations. Using 50 mm as an interval for 3-, 6-, and 12-h rainfall, stations with rainfall amounts of 100–150 mm, 100-150 mm, and

150-200 mm are most common (44.2%, 35.7%, and 27.4%), respectively. Using 100 mm as the interval, stations with 100–200 mm 24-h rainfall are most common, amounting to 44.1% of all stations. These statistics are all comparable to those of corresponding historical maximum rainfall.

Similarly, for various regions labeled in Fig. 1b, the heaviest 50-yr return value for hourly rainfall is about 150 mm over South China. Over the Yellow and Huai River Basin, and the southern North China, the heaviest 50-yr hourly rainfall is about 140 mm. Therefore, there is also only a slight difference in the 50-yr hourly rainfall amounts across these regions. However, for the 50-yr 24-h rainfall, the heaviest rainfall can be above 500 mm over South China; yet it is only above 400 mm over the Yellow and Huai River Basin and less than 400 mm over the southern North China. These results also indicate that the absolute and relative differences in the 50-yr 24-h rainfall between South China and the regions of the Yellow and Huai River Basin and the southern North China is larger than that in 50-yr hourly rainfall.

Rainfall is the product of rainfall rate and duration. But rainfall is also a complex nonlinear physical process, during which rainfall rates are usually non-uniform. Therefore, for any given site, the extreme cumulative rainfall amount in the accumulation period longer than 1 hour almost never equals the extreme hourly rainfall amount multiplied by the number of hours, and its average hourly rainfall intensity is usually less than the extreme hourly rainfall amount. As stated earlier, the regional heaviest historical maximum and the 50-yr hourly rainfall return value over the Yellow and Huai River Basin are close to those over South China, but if we consider the 50-yr rainfall return value at the accumulation periods that are greater than 3 hours, then the differences between these two regions significantly increase as the accumulation period increases. This is because in South China, extreme rainfall tends to last longer (Chen et al. 2013; Li et al. 2013b).

Overall, the results from the historical maximum rainfall and the estimated 50-year return rainfall are consistent to each other.

5. Regional classification and differences in extreme rainfall

a. Regional classification based on extreme rainfall

The similarity between the spatial distribution of the historical maximum rainfall and that of the estimated 50-yr rainfall suggests the reliability of the results obtained in this paper. In this section, we further examine the spatial distributions of extreme rainfall of the three grades, for different accumulation periods.

Based on the maximum extreme rainfall amounts of different grades over each 0.75° × 0.75° grid cell, we present a regional classification in Fig. 6. The main characteristics of the classified regions are summarized below:

1) The extreme rainfall reaching Grade II and Grade III is mainly observed east and south of the black lines in Figs. 4 and 5, which runs from southern Northeast China through Shanxi Province then around the western edge of the Sichuan Basin towards the eastern slope of the Yunnan-Guizhou Plateau, more or less following the terrain elevation contour. However, Grade II is not reached over nearly half of the region between 25°N and 30°N for extreme 3-, 6-, and 12-h rainfall especially.
2) Over Yunnan Province, the eastern Inner Mongolia, and the northern and central Northeast China, there are still a number of cells with Grade II extreme hourly rainfall (no less than 75 mm), but there are fewer cells with Grade II extreme 3-, 6-, 12-, and 24-h rainfall. This shows that over these areas, even if an SDHR event occurs and reaches Grade II extreme hourly rainfall, because of the shorter lifespan of convective

systems producing the rainfall, the cumulative rainfall amounts in longer accumulation periods are less likely to attain Grade II.

3) For different accumulation periods, the spatial distributions of Grade III extreme rainfall are somewhat similar to each other. The similarity is greater among extreme hourly, 3-, and 6-h rainfall, and less so to 12-h and 24-h rainfall.

4) The spatial distributions of Grade III extreme rainfall possess the following characteristics: they are situated over the lower latitudes (e.g., South China), along the southern and eastern coast lines, in the large Yellow and Yangtze River Basins, and over the lower-elevation side of the border region between plains or basins and plateaus or mountains (e.g., the west side of the Sichuan Basin, and the west side of the North China Plain).

5) Both South China and the Sichuan Basin exhibit not only heavier extreme rainfall, but also higher SDHR frequencies (Chen et al. 2013) and more heavy-rainfall days (Zhang and Lin 1985).

6) Between 25°N and 30°N in China, there are fewer cells with Grade III extreme rainfall for different accumulation periods than in the regions of South China, the Yangtze and Huai River Basin, and the Yellow and Huai River Basin. However, there are more cells with Grade III extreme 24-h rainfall than with hourly and 3-h rainfall (Fig. 4e, Fig. 5e and Fig. 6e) over some parts of this region, such as the southern Anhui Province, the eastern Jiangxi Province, and the northwestern Hunan Province. This indicates that, although these regions do not exhibit Grade III extreme hourly rainfall, they can suffer more often from Grade III extreme 24-h rainfall. This phenomenon may be related to their terrain distributions or tropical weather systems such as tropical cyclones that affect

these areas and cause long-duration rainfall.

Rainfall rates in tropical systems are generally high, because they are usually associated with deep moist and organized convection (Davis 2001). The extreme rainfall over South China is often associated with tropical systems that affect this region. Low-level southwesterly jet, land–sea breeze (Zheng et al. 2008; Chen et al. 2015), and differential friction effects between the sea and land (Chen et al. 2014) have been found to provide additional local forcing and trigger for convection and precipitation near the coast. The extreme rainfall over the coastal areas of Zhejiang and Fujian provinces may be related to the frequent influence of tropical cyclones in these areas (Zheng et al. 2014), as well as the land–sea breeze and differential friction effects present along the coast (Chen et al. 2014). The cause for the extreme rainfall over the Yangtze and Huai River Basin, and the Yellow and Huai River Basin, appears to be due to the fact that these areas are situated at the edge of the summer monsoon and the subtropical high in summer so the regions experience long-duration Mei-yu rainfall. From the perspective of convective systems, the regions belong to the active $M_{\alpha}CS$ (Meso-α-scale Convective System) and $M_{\beta}CS$ (Meso-β-scale Convective System) areas (Ma et al. 1997; Zheng et al. 2008), which will also have direct impacts. The extreme rainfall over the Sichuan Basin and the North China Plain should be related to the northward migrating summer monsoon which regularly influences these regions (Chen et al. 1991), as well as the impact of regional terrains. The heavier extreme rainfall for accumulation periods greater than 6 hours may be associated with nocturnal occurrences of heavy rainfall and SDHR over South China, the Sichuan Basin, the Yangtze and Huai River Basin, and the Yellow and Huai River Basin (Chen et al. 2013); and nocturnal rainfall are often associated with MCSs that last longer.

Our study does not try to document seasonal cycles in the extreme rainfall, but they can be a potential focus of future research. As the spatial distribution of rainfall in China is determined primarily by the advance and retreat of the summer monsoon (Tao, 1980; Ding and Zhang 2009), heavy rainfall and SDHR events in China occur most frequently during the summer (June, July, and August), and the second highest heavy rainfall and SDHR frequency in April and May, while their frequency drops substantially in September (Tao 1980; Ding and Zhang 2009; Chen et al. 2013). For various regions, heavy rainfall and SDHR events in South China occur mainly in April, May, June, August, and September; those in the middle and lower reaches of the Yangtze River appear mainly in June, July, and August; and those over North China and Northeast China occur mainly in July and August. Therefore, we can speculate that the extreme rainfall events in China occur mainly in summer, although their seasonal cycles may vary from region to region due to the influence of the summer monsoon. For example, several historically extremely heavy rainfall events occurred in summer, such as those of August 1963 in North China, August 1975 in Henan Province, August 1996 in North China, and July 2012 in Beijing and Hebei Province, all of which caused heavy losses of life and serious damage to property.

b. Differences in extreme rainfall between the south and the north

To highlight the differences in the spatial distributions of extreme rainfall between the south and the north in China, the 30°N parallel is selected (light blue dashed line in Fig. 1) to divide China into the northern and southern regions. Based on the historical maximum rainfall and the 50-yr return values, Fig. 7a presents the comparison of Grade III extreme rainfall with different accumulation periods between these two regions. Figure 7a shows that the percentage of total stations with Grade III extreme rainfall south of 30°N increases significantly as the accumulation period increases, with the percentage increasing from about 49% to about 69% for the historical maximum rainfall, and from about 50% to about 72% for the 50-yr rainfall. In contrast, the percentages over the area north of 30°N significantly decrease as the accumulation period increase, from about 51% to about 31% for the historical maximum rainfall, and from about 50% to about 28% for the 50-yr rainfall.

Similarly, Fig. 7b shows the difference in the percentages of total stations with Grade III extreme rainfall between Guangdong Province and the Beijing–Tianjin–Hebei area (indicated by the light blue solid lines in Fig. 1). Although there are some differences between Fig. 7a and 7b, the trends along with the accumulation period in Fig. 7b for the two local regions are similar to those for the south and north China shown in Fig. 7a. Again, these results show that long duration rainfall events are much more prevalent in the southern part of China, which the occurrence frequencies of hourly extremely rainfall are very similar. The northern and inner parts of China have climates of more continental nature, which are capable of producing intense short-duration convection, but the lack of sustained moisture supply from the ocean tends to limit the duration of heavy rainfall.

6. Summary and conclusions

Based on the hourly rainfall data from 1919 national-level meteorological stations in China during the period of 1981–2012, we first derive the 3-, 6-, 12-, and 24-h running cumulative rainfall, and then estimate the GEV distributions using the hourly and different running cumulative rainfall series. Based on our analysis of these data, we propose a new classification for different accumulation periods to divide the extreme rainfall into three grades. The thresholds separating the three grades correspond to roughly the 70 and 90 percentiles of extreme rainfall. We analyze, compare and classify the spatial distributions of the historical maximum hourly, 3-, 6-, 12-, and 24-h rainfall, and their corresponding estimated 50-yr return values over China.

The coastal areas of the southern and eastern China, the large river basins, the western Sichuan Basin, and the North China Plain all exhibit heavier extreme rainfall for different accumulation periods. Furthermore, both South China and the western Sichuan Basin exhibit not only heavier extreme rainfall, but also higher occurrence frequencies of SDHR and more heavy-rainfall days. In general, the spatial distributions of Grade III extreme hourly, 3-, 6-, 12-, and 24-h rainfall are similar, especially for hourly, 3-, and 6-h rainfall. The distributions of 12- and 24-h rainfall are more different.

The number of stations with Grade III extreme hourly rainfall over the area south of 30°N is nearly as many as that over the area north of 30°N in China. However, when considering the stations with Grade III extreme 6-, 12-, and 24-h rainfall, the differences in the station numbers between these two areas increases significantly as the accumulation period becomes longer. This characteristic reflects that the extreme rainfall intensities of these two areas are almost equal, but the extreme rainfall events over the former area last longer than those over the latter area due to the effects of richer moisture, the low-level southwesterly jet, tropical cyclones, and so on.

The spatial distributions of the 50-yr rainfall using the fitted GEV of static parameters are presented in this paper. They somewhat differ from those of the historical maximum rainfall over certain areas. The differences may be related to the fact that the fitted GEV parameters are static and thus cannot fully reflect climate variabilities in extreme rainfall. In future studies, an alternative method, the Generalized Pareto (GP) distribution, can be explored to investigate long-term trends or climate variabilities in extreme rainfall by defining non-stationary thresholds. Finally, although many studies have investigated the development mechanisms of heavy rainstorms in China (e.g., Tao 1980; Ding and Zhang 2009; Tao and Zheng 2013; Zhao et al. 2013), there remain needs for further research on the weather patterns, the environmental characteristics, and the mesoscale and small-scale mechanisms, of extreme rainfall in China.

Our current study provides only a climatological background for such specific research. Our climatological study, including the classification standards set based on long-term historical data for accumulation periods ranging from hourly through 24-hourly, also has the potential of helping policy makers to draw up region-specific regulations and standards, including those on buildings, roads, reservoirs, dams, and other infrastructures. The standards could also be adopted by the central and regional meteorological services for operational use.

Acknowledgments. We deeply appreciate the constructive comments and suggestions provided by three anonymous reviewers. We would like to acknowledge the National Meteorological Information Center of the China Meteorological Administration for collecting and archiving the hourly rainfall data used in this study. This work was supported by the National Major Basic Research "973" Program of China under 2013CB430100, including its sub-grants 2013CB430106 and 2013CB430103, the Social Common wealth Research Program under grant GYHY201406002, the National Natural Science Foundation of China under grant 41375051, and Key Project of National Social Science Foundation of China (11&zd167).

References

Atomic Energy Regulatory Board of India, 2008: *Extreme Values of Meteorological Parameters*, Mumbai, 37 pp.

Chen, J., Y. Zheng, X. Zhang, and P. Zhu, 2013: Distribution and diurnal variation of warm-season short-duration heavy rainfall in relation to the MCSs in China, *Acta Meteor. Sinica*, **27**, 868–888, doi: 10.1007/s13351-013-0605-x.

Chen, L., Q. Zhu, H. Luo, J. He, M. Dong, and Z. Feng, 1991: *East Asian Monsoon* (in Chinese), China Meteorological Press, Beijing, 362 pp.

Chen, X., K. Zhao, and M. Xue, 2014: Spatial and temporal characteristics of warm season convection over Pearl River Delta region, China, based on 3 years of operational radar data, *J. Geophys. Res. Atmos.*, **119**, 12447–12465, doi: 10.1002/2014JD021965.

Chen, X.-C., K. Zhao, M. Xue, B. Zhou, and W. Xu, 2015: Radar-observed diurnal cycles and propagation of convection over the Pearl River Delta during Mei-Yu season. *J. Geophy. Res. Atm*os., DOI: 10.1002/2015JD023872.

Coles, S., 2001: *An Introduction to Statistical Modeling of Extreme Values*, London: Springer, 223 pp.

Davis, R. S., 2001: Flash flood forecast and detection methods, In *Severe Convective Storms*, *Meteor. Monograph. Amer. Met. Soc.*, **28**, 481–525.

Ding, Y., and J. Zhang, 2009: *Heavy Rain and Flood* (in Chinese), China Meteorological Press, Beijing, 290 pp.

Frich, P., L. V. Alexander, P. Della-Marta, B. Gleason, M. Haylock, AMG Klein Tank, and T. Peterson, 2002: Observed coherent changes in climatic extremes during the second half of the 20th century, *Climate Res.*, **19**, 193–212, doi: 10.3354/cr019193.

Gao, R., X. Zou, and Z. Wang, 2012: *The Atlas of Extreme Weather and Climate Events in China* (in Chinese), China Meteorological Press, Beijing, 188 pp.

Garrett, C., and P. Müller, 2008: Supplement to extreme events, *Bull. Amer. Meteor. Soc.*, **89**, ES45–ES56, doi: 10.1175/2008BAMS2566.2.

Hosking, J. R. M., 1990: L-moments: Analysis and estimation of distributions using linear combinations of order statistics, *J. Roy. Stat. Soc.: B*, **52**, 105–124, DOI: 10.2307/2345653.

IPCC, 2013: *Climate Change 2013: The Physical Science Basis. Contribution of Working Group I to the Fifth Assessment Report of the Intergovernmental Panel on Climate Change* [Stocker, T. F., D. Qin, G. K. Plattner, M. Tignor, S. K. Allen, J. Boschung, A. Nauels, Y. Xia, V. Bex and P. M. Midgley (eds.)]., Cambridge, United Kingdom and New York, NY, USA: Cambridge University Press,1535 pp.

Li, J., R. Yu, and W. Sun, 2013a: Calculation and analysis of the thresholds of hourly extreme precipitation in mainland China (in Chinese), *Torrential Rain and Disasters*, **32**, 11–16, doi: 10.3969/j.issn.1004-9045.2013.01.002.

Li, J., R. Yu, and W. Sun, 2013b: Duration and seasonality of hourly extreme rainfall in the central eastern China, *Acta Meteor. Sinica*, **27**, 799–807, doi: 10.1007/s13351-013-0604-y.

Ma, Y., X. Wang, and Z. Tao, 1997: Geographic distribution and life cycle of mesoscale convective system in China and its vicinity, *Prog. Natur. Sci.*, **7**, 583–589.

Sen Roy, S., 2009: A spatial analysis of extreme hourly precipitation patterns in India, *Int. J. Climatol.*, **29**, 345–355, doi: 10.1002/joc.1763.

Tao, S., 1980: *Heavy Rains in China* (in Chinese), China Science Press, Beijing, 225 pp.

Tao, Z., and Y. Zheng, 2013: Forecasting issues of the extreme heavy rain in Beijing on 21 July 2012, *Torrential Rain and Disasters* (in Chinese), **32**, 193–201, doi: 10.3969/j.issn.1004-9045.2013.03.001.

Zhai, P., A. Sun, F. Ren, X. Liu, B. Gao, and Q. Zhang, 1999: Changes of climate extremes in China, *Climatic Change*, **42**, 203-218, doi: 10.1023/A:1005428602279.

Zhai, P., X. Zhang, H. Wang, and X. Pan, 2005: Trends in total precipitation and frequency of daily precipitation extremes over China, *J. Climate*, **18**, 1096–1107, doi: 10.1175/JCLI-3318.1.

Zhang, H., and P. Zhai, 2011: Temporal and spatial characteristics of extreme hourly precipitation over eastern China in the warm season, *Adv. Atmos. Sci.*, **28**, 1177–1183, doi: 10.1007/s00376-011-0020-0.

Zhang, J. and Z. Lin, 1985: *Climate of China* (in Chinese), Shanghai Science and Technology Press, Shanghai, 436 pp.

Zhao, Y., Q. Zhang, Y. Du, M. Jiang, and J. Zhang, 2013: Objective analysis of circulation extremes during the 21 July 2012 torrential rain in Beijing, *J. Meteor. Res.*, **27**, 626–635, doi: 10.1007/s13351-013-0507-y.

Zheng, Y., J. Chen, and P. Zhu, 2008: Climatological distribution and diurnal variation of mesoscale convective systems over China and its vicinity during summer, *Chinese Sci. Bull.*, **53**, 1574–1586, doi: 10.1007/s11434-008-0116-9.

Zheng, Y., J. Chen, and Z. Tao, 2014: Distributional characteristics of the intensities and extreme intensities of tropical cyclones influencing China, *J. Meteor. Res.*, **28**, 393–406, doi: 10.1007/s13351-014-3050-6.

TABLE 1. The 70th and 90th percentiles of extreme rainfall values for different accumulation periods based on the 1919 extreme rainfall values during 1981–2012

	Rainfall (mm)	
	at 70th percentile	at 90th percentile
Historical maximum hourly rainfall	77.5	96.1
50-yr hourly rainfall	75.4	93.5
Historical maximum 3-h rainfall	127.3	163.9
50-yr 3-h rainfall	124.7	155.9
Historical maximum 6-h rainfall	161.2	212.1
50-yr 6-h rainfall	160.3	202.3
Historical maximum 12-h rainfall	196.4	262.1
50-yr 12-h rainfall	195.8	256.5
Historical maximum 24-h rainfall	232.3	309.4
50-yr 24-h rainfall	229.7	303.6

TABLE 2. Percentiles of the 1919 extreme rainfall values for different levels of extreme rainfall at different accumulation periods during 1981–2012

	Percentiles corresponding to	
Hourly rainfall	75 mm	95 mm
Historical maximum	66	89
50-yr	69	91
	Percentiles corresponding to	
3-h rainfall	125 mm	155 mm
Historical maximum	68	87
50-yr	70	90
	Percentiles corresponding to	
6-h rainfall	160 mm	205 mm
Historical maximum	70	89
50-yr	70	91
	Percentiles corresponding to	
12-h rainfall	195 mm	260 mm
Historical maximum	69	90
50-yr	70	91
	Percentiles corresponding to	
24-h rainfall	230 mm	305 mm
Historical maximum	69	89
50-yr	70	90

TABLE 3. Grades of extreme rainfall defined in this study for different accumulation periods (R denotes rainfall amounts in the table)

	Rainfall (mm) of different grades		
	Grade I	Grade II	Grade III
Extreme hourly rainfall	< 75	$75 \leqslant R < 95$	≥ 95
Extreme 3-h rainfall	< 125	$125 \leqslant R < 155$	≥ 155
Extreme 6-h rainfall	< 160	$160 \leqslant R < 205$	≥ 205
Extreme 12-h rainfall	< 195	$195 \leqslant R < 260$	≥ 260
Extreme 24-h rainfall	< 230	$230 \leqslant R < 305$	≥ 305

LIST OF FIGURES

FIG. 1. China topography (a), and locations of those stations with continuous observations of hourly rainfall for 1965–2012 (orange dots) and for 1981–2012 (green dots) (b). (In Fig. b, thick solid lines separate various regions marked by numbers: ① - South China; ② - the coastal areas of Fujian and Zhejiang provinces; ③ - Guizhou and Hunan provinces, and the most part of Jiangxi Province; ④ - eastern Jiangxi Province and the inland areas of Fujian and Zhejiang provinces; ⑤ - the Sichuan Basin; ⑥ - Hubei Province; ⑦ - the Yangtze and Huai River Basin; ⑧ - the Yellow and Huai River Basin; ⑨ - the Shandong Peninsula; ⑩ - the North China Plain; ⑪ - the southern Liaoning Province.)

FIG. 2. Probability plots (a, b, e, f) and fitted GEV distributions (c, d, g, h) of hourly (a, b, c, d) and 24-h (e, f, g, h) rainfall at Beijing station based on 1965–2012 (a, c, e, g) data and 1981–2012 data (b, d, f, h). (Blue lines in c, d, g, and h indicate the 95% confidence intervals. Note that the vertical coordinate ranges in c, d, g, and h are different and unit is mm)

FIG. 3. As in Fig. 2, but for Qingyuan station in Guangdong Province.

FIG. 4. Color-filled contour maps of historical maximum (a) hourly, (b) 3-, (c) 6-, (d) 12-, and (e)

24-h rainfall at 1919 stations in China for 1981–2012 (units: mm), mapped to a 0.75° latitude-longitude grid. The dark blue and magenta colors correspond to Grade II and Grade III of extreme rainfall, respectively, while three lower thresholds are also plotted. The stations with Grade II and Grade III extreme rainfall are marked by green triangles and yellow dots, respectively (see legends). The thick black line in each panel marks the western boundary of stations that ever recorded Grade III extreme rainfall events (hourly rainfall of ≥ 95 mm, 3-h rainfall of ≥ 155 mm, 6-h rainfall of ≥ 205 mm, 12-h rainfall of ≥ 260 mm, or 24-h rainfall of ≥ 305 mm)

FIG. 5. As in Fig. 4, but for estimated 50-yr rainfall using the GEV distribution: (a) hourly rainfall; (b) 3-h rainfall; (c) 6-h rainfall; (d) 12-h rainfall; (e) 24-h rainfall.

FIG. 6. Regional classification based on historical maximum and 50-yr rainfall amounts: (a) hourly rainfall; (b) 3-h rainfall; (c) 6-h rainfall; (d) 12-h rainfall; (e) 24-h rainfall (units: mm). White areas indicate no rainfall observation, and red areas indicate historical maximum rainfall reaching Grade III and 50-yr rainfall under Grade III.

FIG. 7. Comparison of the percentages of the total stations with Grade III extreme rainfall over:

(a) South and north of 30°N in China; (b) Beijing–Tianjin–Hebei area and Guangdong Province. Vertical axis: percentage (%); horizontal axis: accumulation period (h).

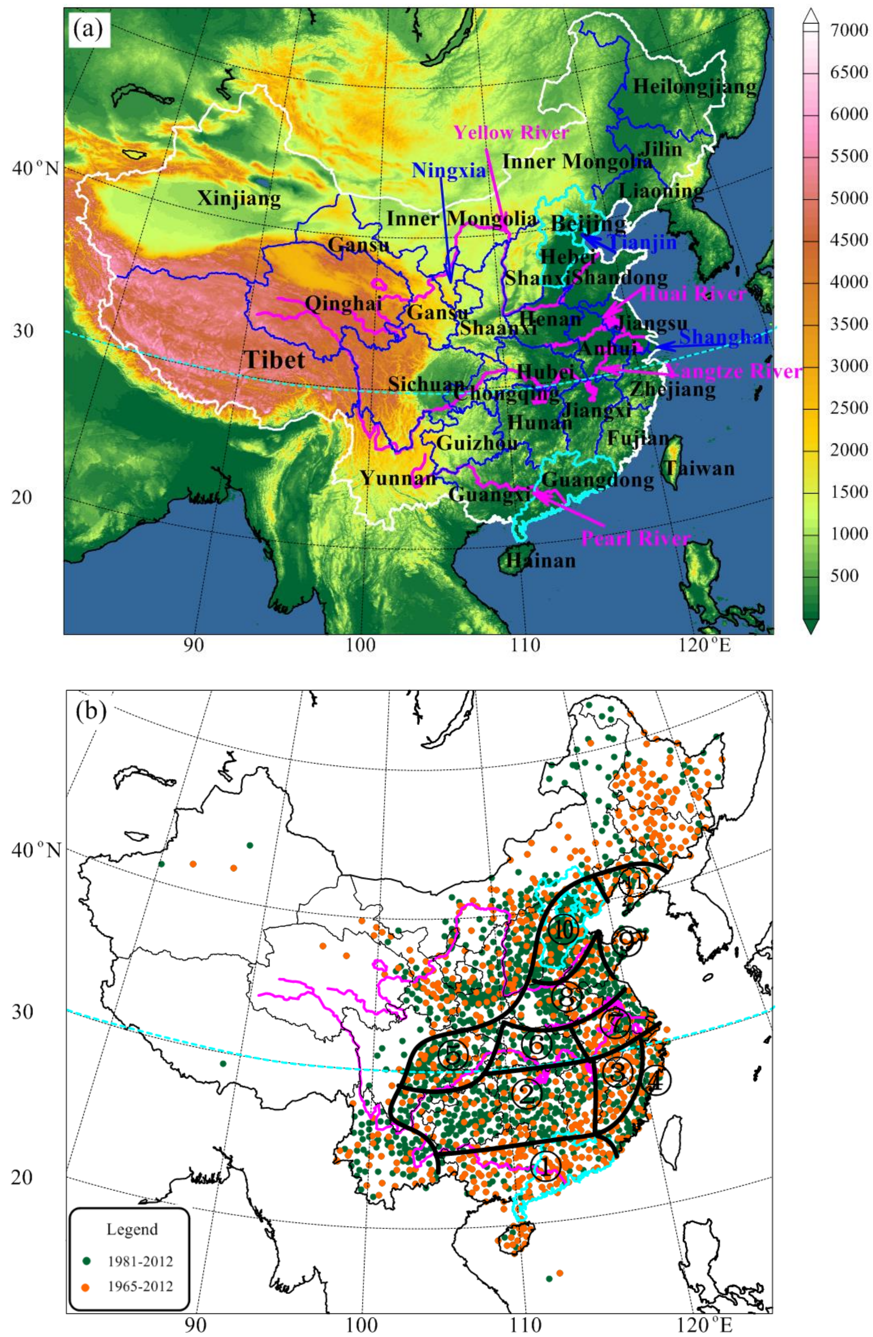

FIG. 1. China topography (a), and locations of those stations with continuous observations of hourly rainfall for 1965–2012 (orange dots) and for 1981–2012 (green dots) (b). (In Fig. b, thick solid lines separate various regions marked by numbers: ① - South China; ② - the coastal areas of Fujian and Zhejiang provinces; ③ - Guizhou and Hunan provinces, and the most part of Jiangxi Province; ④ - eastern Jiangxi Province and the inland areas of Fujian and Zhejiang provinces; ⑤ - the Sichuan Basin; ⑥ - Hubei Province; ⑦ - the Yangtze and Huai River Basin; ⑧ - the Yellow and Huai River Basin; ⑨ - the Shandong Peninsula; ⑩ - the North China Plain; ⑪ - the southern Liaoning Province.)

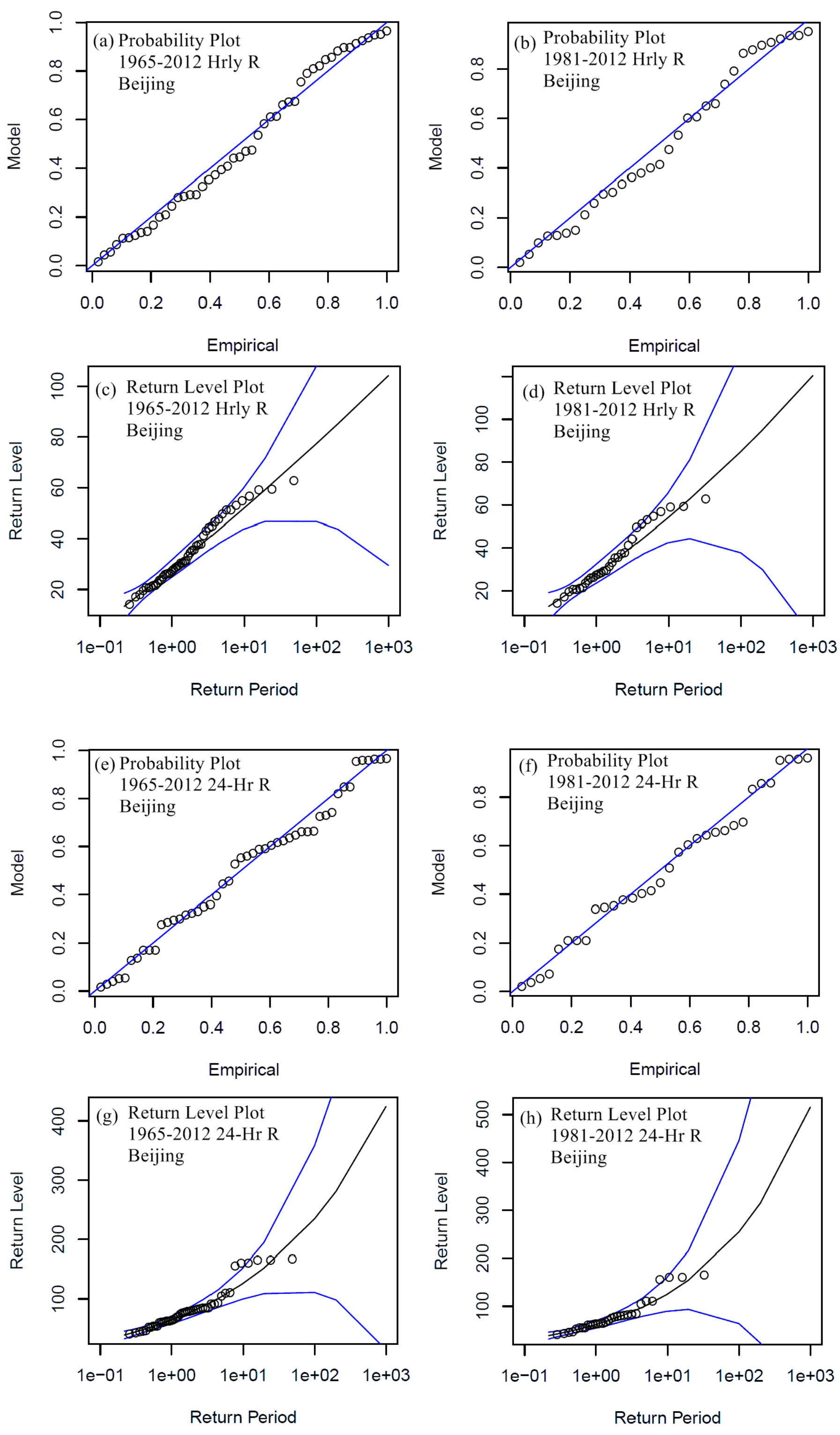

FIG. 2. Probability plots (a, b, e, f) and fitted GEV distributions (c, d, g, h) of hourly (a, b, c, d) and 24-h (e, f, g, h) rainfall at Beijing station based on 1965–2012 (a, c, e, g) data and 1981–2012 data (b, d, f, h). (Blue lines in c, d, g, and h indicate the 95% confidence intervals. Note that the vertical coordinate ranges in c, d, g, and h are different and unit is mm)

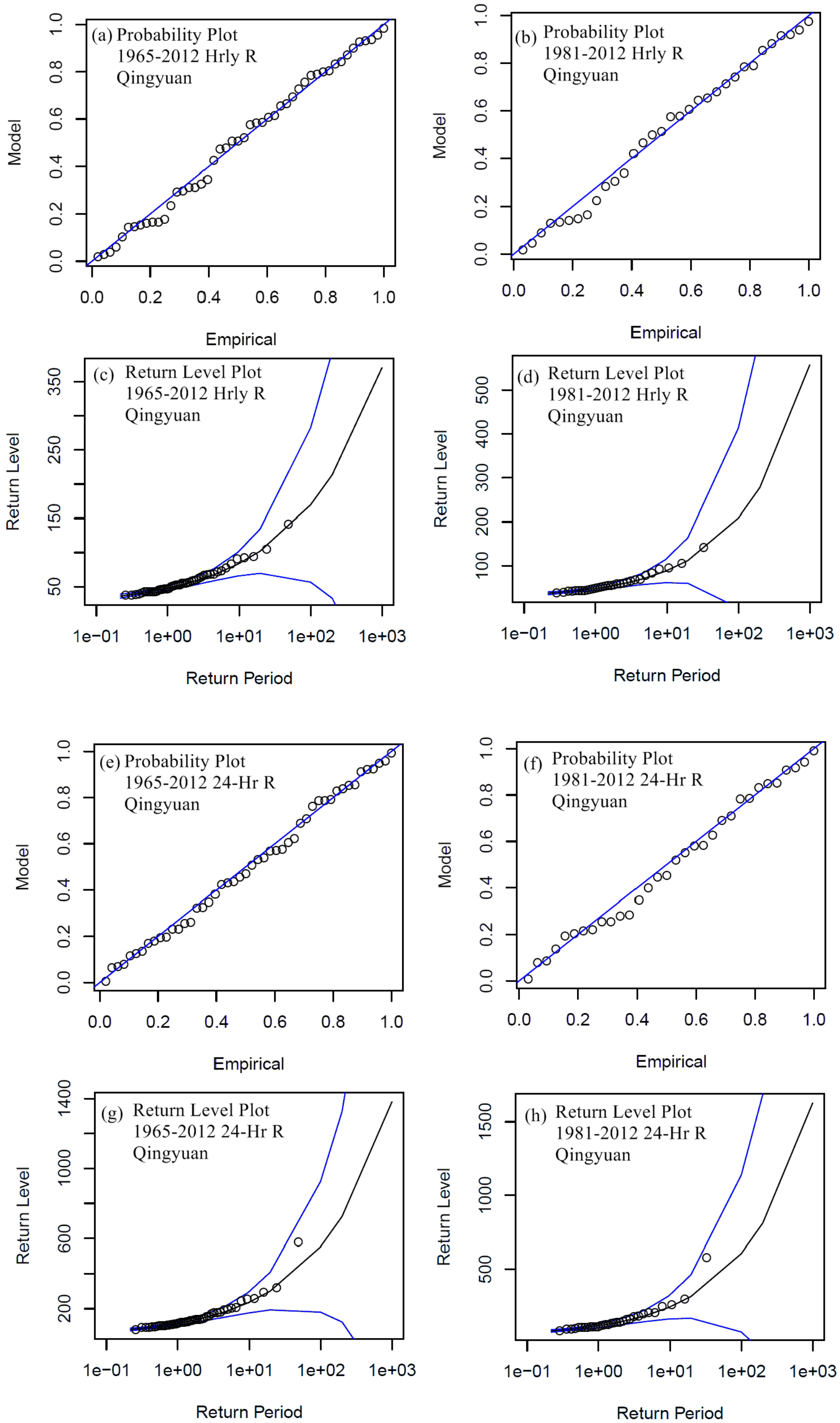

FIG. 3. As in Fig. 2, but for Qingyuan station in Guangdong Province.

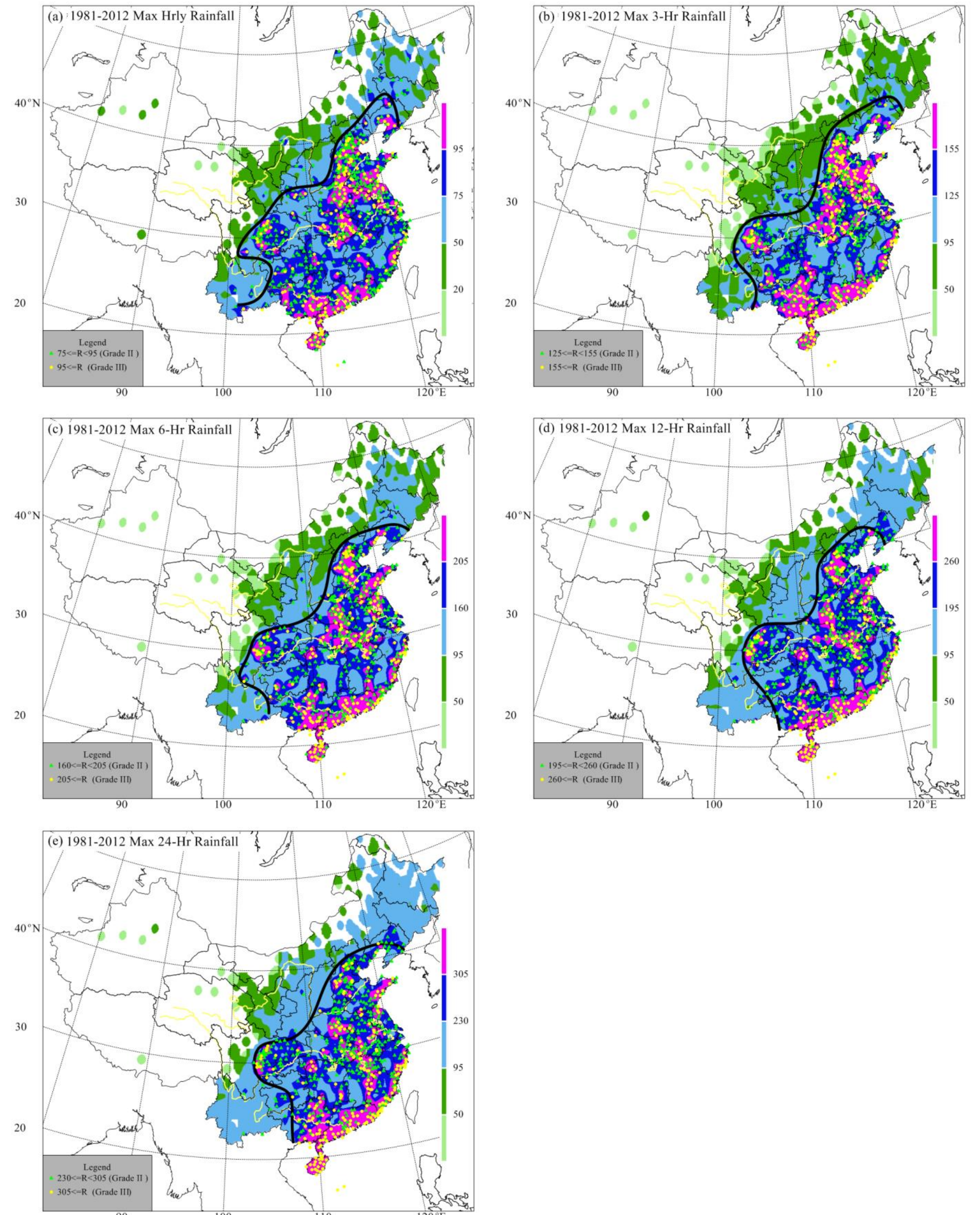

FIG. 4. Color-filled contour maps of historical maximum (a) hourly, (b) 3-, (c) 6-, (d) 12-, and (e) 24-h rainfall at 1919 stations in China for 1981–2012 (units: mm), mapped to a 0.75° latitude-longitude grid. The dark blue and magenta colors correspond to Grade II and Grade III of

extreme rainfall, respectively, while three lower thresholds are also plotted. The stations with Grade II and Grade III extreme rainfall are marked by green triangles and yellow dots, respectively (see legends). The thick black line in each panel marks the western boundary of stations that ever recorded Grade III extreme rainfall events (hourly rainfall of ≥ 95 mm, 3-h rainfall of ≥ 155 mm, 6-h rainfall of ≥ 205 mm, 12-h rainfall of ≥ 260 mm, or 24-h rainfall of ≥ 305 mm).

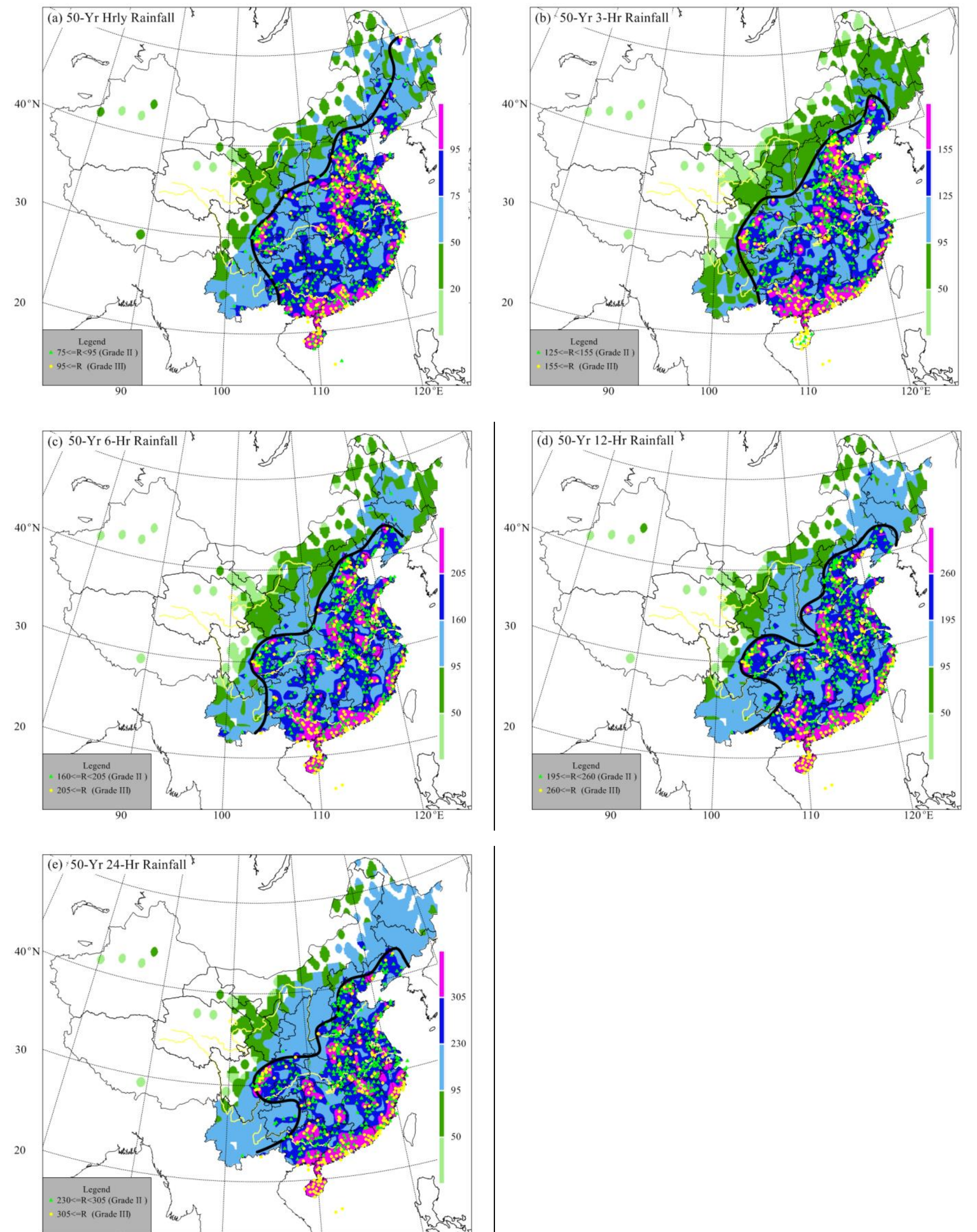
(a) 50-Yr Hrly Rainfall
Legend
75<=R<95 (Grade II)
95<=R (Grade III)
95
75
50
20
(b) 50-Yr 3-Hr Rainfall
Legend
125<=R<155 (Grade II)
155<=R (Grade III)
155
125
95
50
(c) 50-Yr 6-Hr Rainfall
Legend
160<=R<205 (Grade II)
205<=R (Grade III)
205
160
95
50
(d) 50-Yr 12-Hr Rainfall
Legend
195<=R<260 (Grade II)
260<=R (Grade III)
260
195
95
50
(e) 50-Yr 24-Hr Rainfall
Legend
230<=R<305 (Grade II)
305<=R (Grade III)
305
230
95
50
40°N
30
20
90
100
110
120°E

FIG. 5. As in Fig. 4, but for estimated 50-yr rainfall using the GEV distribution: (a) hourly rainfall; (b) 3-h rainfall; (c) 6-h rainfall; (d) 12-h rainfall; (e) 24-h rainfall.

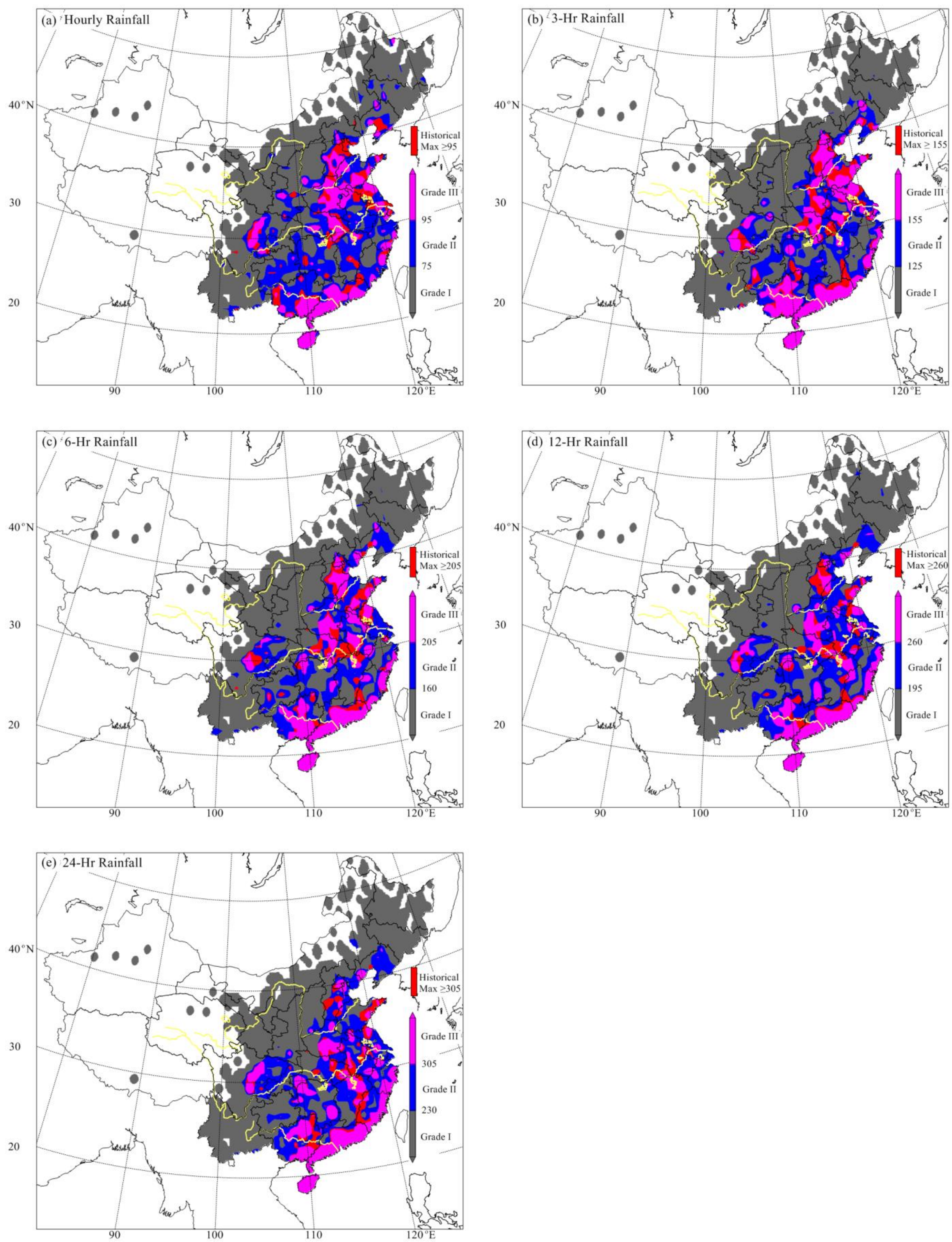

FIG. 6. Regional classification based on historical maximum and 50-yr rainfall amounts: (a) hourly rainfall; (b) 3-h rainfall; (c) 6-h rainfall; (d) 12-h rainfall; (e) 24-h rainfall (units: mm). White areas indicate no rainfall observation, and red areas indicate historical maximum rainfall reaching Grade III and 50-yr rainfall under Grade III.

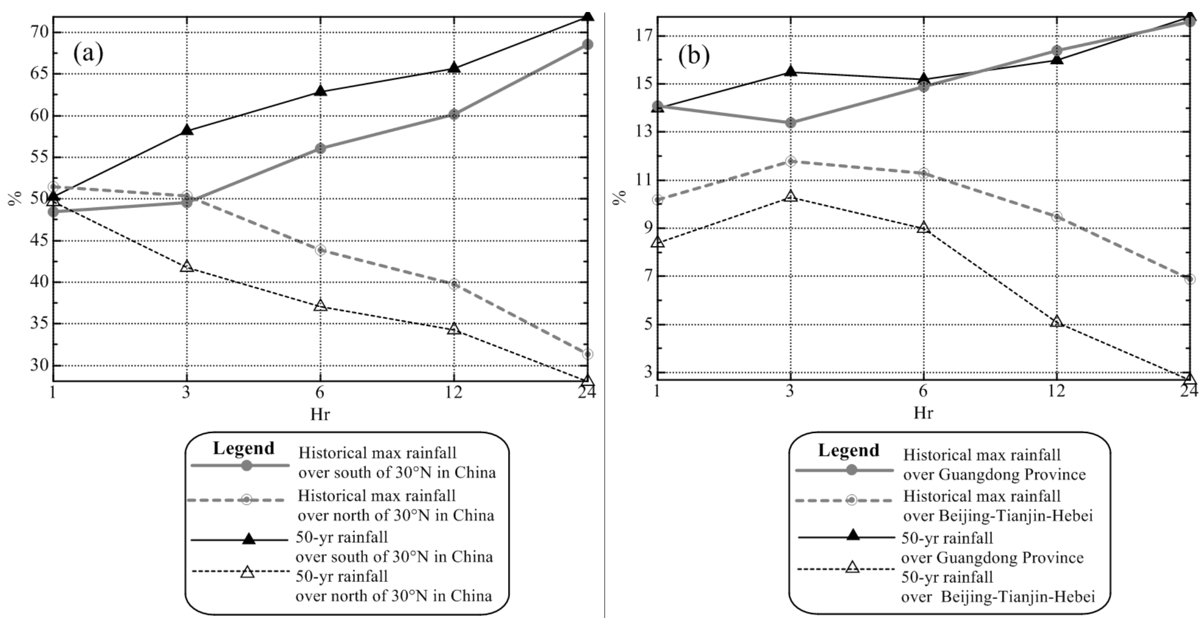

FIG. 7. Comparison of the percentages of the total stations with Grade III extreme rainfall over: (a) South and north of 30°N in China; (b) Beijing–Tianjin–Hebei area and Guangdong Province. Vertical axis: percentage (%); horizontal axis: accumulation period (h).